ISSN 2347 - 3983
Volume 8. No. 5, May 2020
International Journal of Emerging Trends in Engineering Research
Available Online at http://www.warse.org/IJETER/static/pdf/file/ijeter42852020.pdf
https://doi.org/10.30534/ijeter/2020/42852020

Effect of electromagnetic parameters of the medium on the GPR data

Mohammed Hamdaoui, Ahmed Faize, Majid Rochdi, Gamil Alsharahi
Department of Physics, Polydisciplinary Faculty of Nador, Mohammed First University, Morocco
hamdawimohammedpc@gmail.com, ahmedfaize6@hotmail.com, m.rochdi@ump.ac.ma,
alsharahigamil@gmail.com

ABSTRACT

The contrast of dielectric permittivity is very necessary for the detection of objects by ground penetration radar (GPR). The objective of this work is to study the effect of dielectric permittivity on signal quality (GPR). For our simulations scenario, two frequencies are used, 800 MHz to probe three targets of different electrical properties in a homogeneous geological environment, and 1600 MHz for two blocks of concrete with different conditions in terms of relative permittivity and humidity. We discuss the results obtained for predicting the effect of the dielectric constant on the anomalies identified by the GPR. Reflexw is a software, based on the FDTD numerical method, is one of the geophysical processing and interpretation software available for the design and simulation of the various models studied. Finally, through our simulation results and field experiments, we concluded that the value of permittivity is primarily dependent on water content, which has a significant impact on the rate of propagation, as well as on the attenuation of the reflected energy due to absorption and reflection in the different components of geological environments.

Key words: Ground penetration radar, Propagation, Electromagnetic wave. Relative permittivity.

1. INTRODUCTION

The objective of this ground penetration radar (GPR) study is to use short electromagnetic pulses from an emitting antenna coupled to the ground, these pulses propagate in the different layers of heterogeneous media (geological or geotechnical), some of whose energy is reflected in the interfaces of buried materials, which can be a conductor, dielectric or combination of the two, to return to the receiving antenna for the interpretation of the signal, while the other penetrate deeper. This technique has great potential and is commonly used in civil engineering, mapping, geological and geotechnical studies, and the in civil engineering. [1], [2], [17]

GPR data (electromagnetic wave) may be affected during transmission and reflection by the physical properties $(\sigma, \varepsilon \; and \; \mu)$ of the surveyed media. The phase (polarity of the wave) and the amplitude of reflection are indicators of the nature of the buried materials. This condition will be checked by the Reflexw software, which will allow us to simulate 2D numerical simulation based on its electrical and magnetic parameters to understand its spatial organization. The software is based on the Finite Differences Method in the Temporal Domain (FDTD). The main advantages for using the FDTD method are its ease of implementation in a computer program and its flexibility in relation to other methods of electromagnetic modeling such as finite and integral element techniques [3]. This technique allows to measure the contrast of the electrical characteristics of the subsurface materials by local resolution of Maxwell equations, moving the radar to the ground surface to obtain traces (B-scans) on a time window, and thus reduce the nature and spatial distribution of these target materials.

The purpose of this study is to understand the effect of dielectric permittivity and conductivity of the environments crossed by GPR on the quality of the amplitude of the electromagnetic waves reflected, transmitted and\or refracted between the transmitter and the receiver[16]. Simulations by Reflexw software were designed to analyze the inconsistent echo of the receiving antenna under different dielectric constants, using a bi-static antenna network [1], [5], [2], [4]. Models designed under different conditions in terms of relative permittivity and humidity include, on the one hand, a plastic tube, an iron bar and a bottle of fresh water buried in a homogeneous geological environment with a simulation frequency set at 800MHz, on the other hand buried the same objects in a 30 cm thick dried concrete slab whose relative permittivity is variable because of the water content with a frequency fixed at 1600MHz,in order to compare the simulations with experimental results.

The permittivity has a significant impact on the speed of propagation and on the reduction of electromagnetic energy due to absorption and reflection in the various constituents of geological environments.

2. MATERIAL AND THEORY

2.1. Principle of the GPR technique

The operating principle of ground penetration radar (GPR) systems is to emit a short electromagnetic pulse (EM) through the emission antenna in the microwave range (0,1GHz to 2,6 GHz). Thus, the radar waves propagate in the ground with a speed that depends on the physical properties of the media, the receiving antenna measures the amplitude of the electric fields generated by the objects (targets) located in its environment according to the time. The Amplitude-Time signal thus recorded is usually called A-scan(Figure 1(a)). These signals recorded in a space step fixed by the operator arefirstconvertedto color level and then juxtaposed to generate a radar time cut (B-scan)(Figure 1(b)).

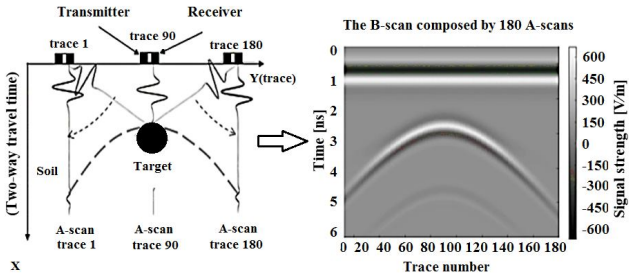

(a) (b)

Figure 1: Schematic diagram of the acquisition of GPR. (a): The Amplitude-Time signal (A-Scan). (b): radar time cutter (B-scan)

2.2. Numerical modelling of GPR: Finite-difference time domain method

The FDTD method (finite differences in the temporal domain) is based on the local resolution of the two Maxwell-Faraday and Maxwell-Ampère equations, which describe the electric and magnetic fields resulting from the distribution of electric loads and currents. The propagation of electromagnetic fields is governed by the Maxwell's equations (1) and (2) [1], [9].

$$\frac{\partial \vec{E}(r,t)}{\partial t} = \frac{1}{\varepsilon_r}\left[\left(\vec{\nabla} \times \vec{H}(r,t)\right) - \sigma\vec{E}(r,t)\right] = \frac{1}{\varepsilon_r}\left[\left(\vec{\nabla} \times \vec{H}(r,t)\right) - \vec{J}(r,t)\right] \quad (1)$$

$$\frac{\partial \vec{H}(r,t)}{\partial t} = -\frac{1}{\mu_r}\left[\vec{\nabla} \times \vec{E}(r,t)\right] \quad (2)$$

$$\vec{B}(r,t) = \mu_r.\vec{H}(r,t) \quad (3)$$

$$\vec{D}(r,t) = \varepsilon_r.\vec{E}(r,t) \quad (4)$$

Where$\vec{E}$ is the electric field in V/m,
$\vec{H}$ isthe magnetic field in A/m,
$\vec{J}$is the total electrical current density in A/m^2
$\vec{B}$is the magnetic flux density in $V.s/m^2$,
$\vec{D}$ is the electric flux density in $A.s/m^2$

The FDTD approach allows the different systems to be modeled in the basement based on a double spatial and temporal discretization of the systems being studied. The mesh size should always be finite and as small as possible in order to properly describe the geometry of the internal structures of geological models. The pioneering work of Yee in 1966 [3]simplified the FDTD algorithm, based on the principle of centered derivatives, which requires that electrical and magnetic components be evaluated in space and time, the temporal evolution of these fields describes the propagation of an electromagnetic wave in the simulated environment [9]. The 3D Yee cell is shown in Figure 2. The 2D FDTD cell is easily obtained by simplifying the 3D Yee cell.

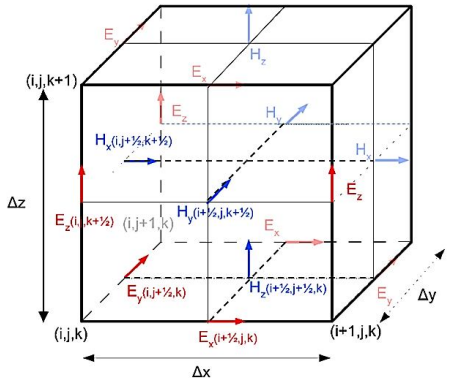

Figure 2: The Yee cell 3D.

The peculiarity of this scheme is to calculate the components of the electric field $\vec{E}$ and magnetic field $\vec{H}$ moved by a half-cell in space, and a half-step in time. The solution is obtained iteratively, so that a field component at a position (x, y, z) and at time t is defined by $(x = i\Delta x, y = j\Delta y, k\Delta z, t = n\Delta t)$. In each iteration, the electromagnetic fields advance (propagate) in the FDTD grid and each iteration corresponds to a simulated elapsed time of an Δt, such that the components of the magnetic field $\vec{H}$ are calculated at the instants $(t + n\Delta t)$, while those of the electric field $\vec{E}$ are calculated at the instants $(t + 1/2\, n\Delta t)$. For the transverse electric (TE) mode, the 2D FDTD equations become [6],[8],[10].

$$E_x\big|_{i,j,k}^{n+\frac{1}{2}} = \frac{1}{\frac{\varepsilon_{i,j,k}}{\Delta t}+\frac{\sigma_{i,j,k}}{2}}\left[\left(\frac{-H_y\big|_{i,j,k+\frac{1}{2}}^{n+\frac{1}{2}} + H_y\big|_{i,j,k-\frac{1}{2}}^{n+\frac{1}{2}}}{\Delta z}\right) + \left(\frac{\varepsilon_{i,j,k}}{\Delta t} - \frac{\sigma_{i,j,k}}{2}\right) E_x\big|_{i,j,k}^{n}\right] \quad (3)$$

$$E_y\big|_{i,j,k}^{n+\frac{1}{2}} = \frac{1}{\frac{\varepsilon_{i,j,k}}{\Delta t}+\frac{\sigma_{i,j,k}}{2}}\left[\left(\frac{H_x\big|_{i,j,k+\frac{1}{2}}^{n+\frac{1}{2}} - H_x\big|_{i,j,k-\frac{1}{2}}^{n+\frac{1}{2}}}{\Delta z}\right) + \left(\frac{\varepsilon_{i,j,k}}{\Delta t} - \frac{\sigma_{i,j,k}}{2}\right) E_y\big|_{i,j,k}^{n}\right] \quad (4)$$

In our simulation we can calculate the electric field $\vec{E}$ as a function of the magnetic field B in the cell of Yee from equations (3) and (4), using discretization $\Delta x = \Delta y = \Delta z = 5\,mm$, while the size of the domain is 800 ×800 ×400 cells [9].

2.3. Propagation velocity and reflection coefficient

The radar propagation speed $v$is different for each medium geological (non-magnetic medium $\mu_r = \mu/\mu_0 = 1$). It is defined by the relation:

$$v = \frac{c}{\sqrt{\varepsilon_r}} = \frac{0.3}{\sqrt{\varepsilon_r}} = \frac{z}{t} \qquad (5)$$

Where z is the target depth in (m),
c is the velocity of electromagnetic waves in air in (m/ns)
$\varepsilon_r$is the relative dielectric permittivity of the medium,
t is the approximate delay time for the reflected signal in (ns)

Most GPR radars use waves that are linearly polarized and then further subdivided into perpendicular or parallel polarization. The reflection (Figure 3) depends on the electromagnetic contrast they encounter, for the TE mode we have:

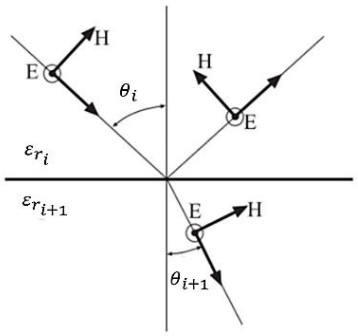

Figure 3: Reflected and transmitted waves in the case of a flat interface for TE mode

The reflection coefficient describes the amount of radar energy reflected by an interface separating two materials with different physical properties, its expression is determined by the contrast of dielectric permittivity; this coefficient is given for the TE mode by the following relation [7,13]:

$$\Gamma_{i\to i+1}^{TE} = \frac{\sqrt{\varepsilon_{r_i}}\cos\theta_i - \sqrt{\varepsilon_{r_{i+1}}}\cos\theta_{i+1}}{\sqrt{\varepsilon_{r_i}}\cos\theta_i + \sqrt{\varepsilon_{r_{i+1}}}\cos\theta_{i+1}} \qquad (6)$$

Where is theε_{r_i}Relative dielectric permittivity of medium i, $\varepsilon_{r_{i+1}}$is therelative dielectric permittivity of medium $i+1$.

When the EM wave is incident vertically on the interface $\theta_1 = \theta_2 = 0$ (radar with an air-coupled antenna), the reflection coefficient can be simplified to:

$$\Gamma_{i\to i+1}^{TE} = \frac{\sqrt{\varepsilon_{r_i}} - \sqrt{\varepsilon_{r_{i+1}}}}{\sqrt{\varepsilon_{r_i}} + \sqrt{\varepsilon_{r_{i+1}}}} \qquad (7)$$

2.4. Electrical conductivity and permittivity

The dielectric properties and conductivity depend on the composition of the materials. Thus, the electrical conductivity (in mS/m) increases with frequency, which partly explains the reduction of the depth of investigation when frequency increases, this effect is responsible for the attenuation of the wave in the propagation medium, the maximum depth of investigation $Z(m)$ by the radar can be estimated by the relationship: [15],[17].

$$Z = \sqrt{\frac{1}{\pi f \mu_0 \sigma}} \approx 503\sqrt{\frac{1}{f\sigma}} \qquad (8)$$

Where$Z$ is the depth of penetration in (m),
σ is the electrical conductivity in(mS/m),
μ_0 is the magnetic vacuum permeability in ($\mu_0 = 4\pi.10^{-7}\,H/m$),
$f$is the frequency of the electromagnetic wave (MHz).

In order to explain the influence of the contrast between the dielectric properties of materials which determines the intensity of the reflection of radar waves at the interfaces between materials, we propose the study a homogeneous model which correctly models most soils at several relaxation times, with a frequency-dependent permittivity, Cole-Cole [16] have shown that the permittivity ε can be calculated using the following relation:

$$\varepsilon(f) = \varepsilon_\infty - \frac{\varepsilon_s - \varepsilon_\infty}{(1+2\pi j f\tau)^{1-\alpha}} - j\frac{\sigma(0)}{2\pi f \varepsilon_0} \qquad (9)$$

where: $\varepsilon(f) = \varepsilon'(f) - j\varepsilon''(f)$: Complex permittivity.
ε_∞: Permittivity at high frequency.
ε_s : Permittivity at low frequency.
f: frequency $[Hz]$.
τ: relaxation time $[s]$.
$\sigma(0)$: DC conductivity $[S/m]$.
α: Depreciation factor, with $0 \le \alpha \le 1$.
$j^2 = -1$ and $\varepsilon_0 = 8{,}854.10^{-12}[F/m]$.

Table 1: Physical properties of materials

Material	Relative permittivity	Conductivity (S/m)	EM wave speed (m/ns)
Air	1	0	0,30
Clay	19	0.1	0,068
Saturated sand	30	0.001	0.054
Concrete	6	0,001	0,12
Freshwater	81	0.01	0,033
Plastic	4.5	0.0004	0.14
Iron	1.45	$9.98.10^6$	0,249
Sands (dry)	4	0.00001	0,15

3. RESULTS AND DISCUSSION

3.1. Simulation by REFLEXW software to study the effect of relative permittivity on the quality of GPR signals (Antenna 800MHZ)

In order to study the impact of dielectric properties on radar energy reflected by an interface separating two materials with different physical properties, we propose in this section a simulation comparison under the Reflexw software of three models, with different permittivity materials (Dielectric, conductor and cavity) buried in homogeneous media at a depth of 0.5 m. The results are discussed and analyzed for each case.

A. *Buried plastic tube*

A plastic tube of relative permittivity $\varepsilon_r = 4.5$ has a very low conductivity$\sigma = 0.00004\ S/m$ is buried at a depth of 0.5 m (Fig.4a). The simulation domain is modeled with dry sand ($\varepsilon_r = 4$; $\sigma = 0.00001\ S/m$ and v=$0.15 m/ns$).In the Radar gram obtained (Fig.4c) a single hyperbola is observed with a peak at 0.5m.

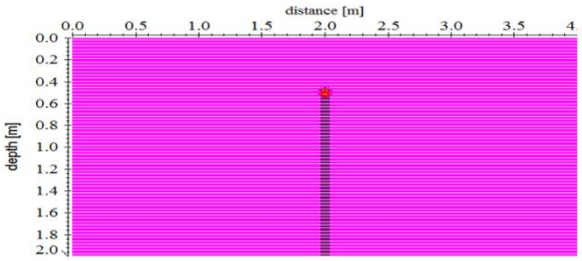

Figure 4:(a) Modelling a plastic pipe buried in a dry sand medium at a depth of 0.5m, for f = 800MHz.

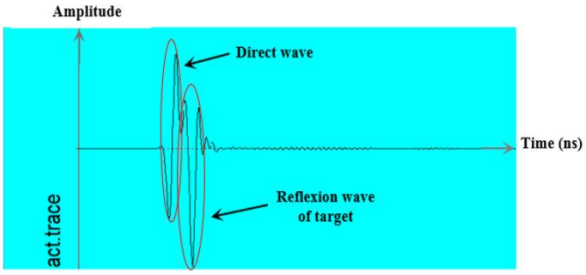

Figure 4:(b) Radargram of the plastic pipe detected using Reflexw: wave evolution over time, for f = 800MHz.

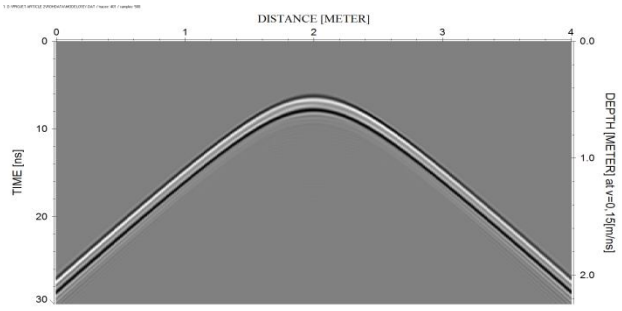

Figure 4:(b) Radargram of the plastic pipe detected using Reflexw, for f = 800MHz.

B. *Buried iron bar*

To carry out the simulation, in this case the ground in which the bar is buried is always simulated by dry sand with dielectric characteristics ($\varepsilon_r = 4, \sigma = 0.00001\ S/m$, and $v = 0.15 m/s$). The iron bar has a conductivity $\sigma = 9.93\ 10^6\ S/m$ and a relative permittivity$\varepsilon_r = 1.45$. The results obtained are displayed in figure 5. In this Figure, we notice the presence of two diffraction hyperbolas which indicate the presence of an iron bar at a depth of 0.5m (i.e. exactly the depth at which it was supposed to be buried).

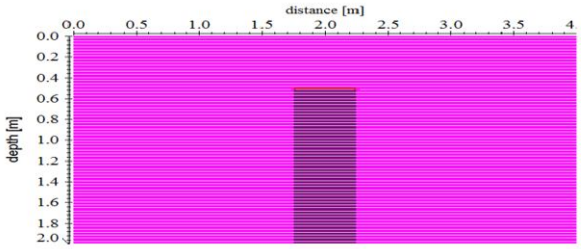

Figure 5: (a) Modeling an iron bar buried in a concrete environment at a depth of 0.5 m, for f = 800MHz.

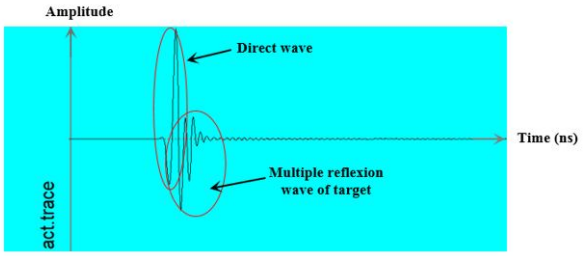

Figure 5:(b) Radargram of the iron bar detected using Reflexw: wave evolution over time, for f = 800MHz.

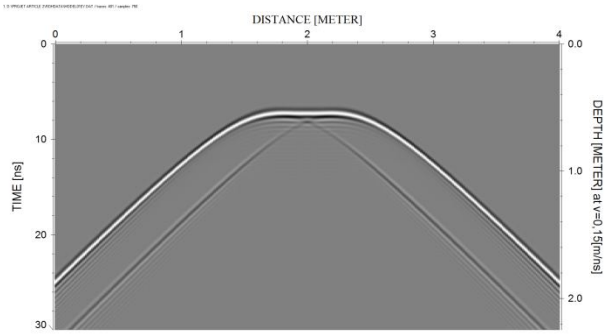

Figure 5: (c) Radargram of the iron bar detected using Reflexw, for f = 800MHz.

C. *Buried freshwater bottle*

In this case the simulation was carried out in dry sand where a plastic bottle containing water was buried at the same depth of 0.5 m. The freshwater bottle has a high relative permittivity ($\varepsilon_r = 81$; $\sigma = 0.0005\ s/m$) which decreases the speed of propagation of the electromagnetic waves, consequently a delay appears in the backscattered wave collected by the receiving antenna. This delay generates several hyperbolas corresponding to several consecutive reflections but at different times for the frequency used (800 MHz) Fig. 6 (c).

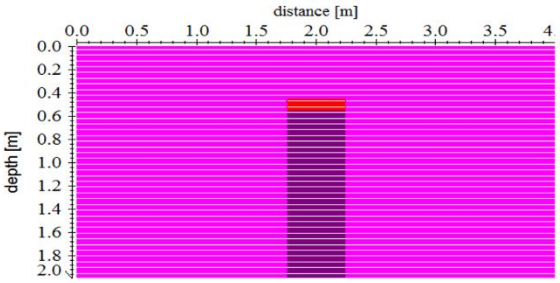

Figure 6: (a) Modelling of a water bottle buried in a dry sand environment, for f = 800MHz.

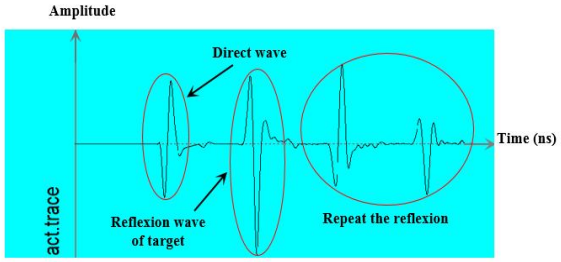

Figure 6:(b) Radargram of the plastic pipe detected usingReflexw: wave evolution over time, for f = 800MHz.

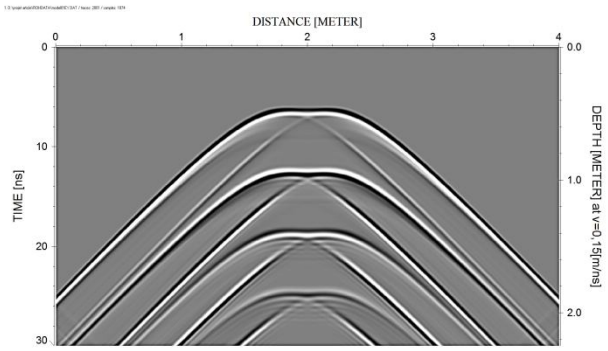

Figure 6: (c) Radargram of the water bottle detected using Reflexw, for f = 800MHz.

3.2. Laboratory experiment to study the effect of relative permittivity on GPR signal quality (Antenna 1600MHz)

The study presented in this paragraph aims to estimate the influence of dielectric permittivity of concrete base on water content on the quality of the signals reflected by buried objects, two armed steel bars and two plastic tubes (PVC) buried in dried concrete base (Figure 7), with different conditions in terms of relative permittivity (6-30) due to the hydration of the concrete base. The measurements were carried out in different stages of time with a 7-day increment on both tiles. Raw measurements (unprocessed B-scans) recorded by the GPR radar are compared and analyzed, and then improved by digital image processing on the Reflexw to eliminate noise from the results.

(a) (b)

Figure 7: (a): two bars of iron leaking into a concrete block (b): two bars of plastic leaking into a concrete block

A. *Buried iron bars in concrete base*

We two $10mm$ diameter reinforced steel bars into a dried concrete slab with a relative permittivity that is variable due to the water content $(6 < \varepsilon_r < 30)$, with a conductivity equal to $\sigma = 0.001\, S/m$ and with a permeability $\mu = 1$. he two bars are placed at a distance of $200\, mm$ from each other and buried at a depth of $8\, cm$from the scanning surface, we carry out each study with a 7-day increment during the first three weeks and record the results (Figure 8) at each stage, with a frequency set at 1600MHz.

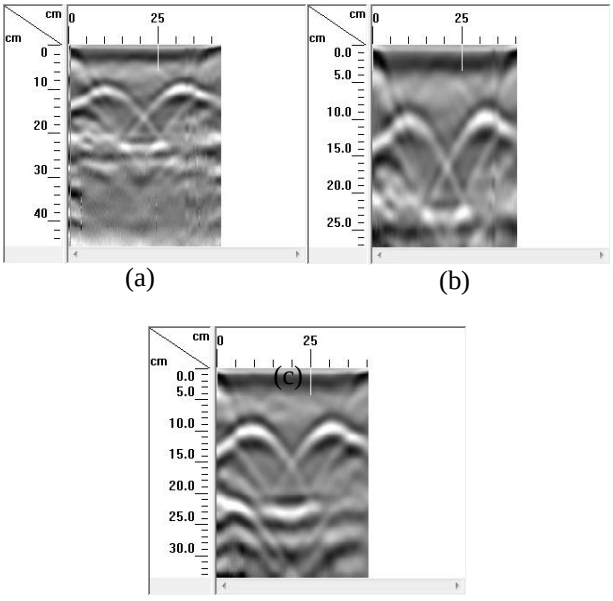

Figure 8: Radargrams of the two iron bars trapped in a concrete block; for f = 1600MHz;
(a): experimental with relative permittivity $\varepsilon_r = 30$ (7-day);
(b): $\varepsilon_r = 15$ (14-day); (c): $\varepsilon_r = 6$ (21-day)

Data recorded by reflections on iron bars, showed a decrease in permittivity based on time since manufacture. For the various B-scans in Figure 8, we notice a reduction in contrast of the image of GPR with increase in water content. Indeed, the water content has the effect of increasing the dielectric constant of concrete base. The presence of water during the first days of the radar inspection radius the speed propagation the of EM wave, which radius the scans quality. In addition, high hydration increases the conductivity of concrete, which penalizes radar measurements because the

signal is more attenuated than transmitted (Figure 8 (a)). After 14 days, and then the hydration of concrete decreases, a remarkable decrease in the dielectric constant (ε_r = 15), the hyperbole (Figure 8(b)) become a little more clear. After 21 days of manufacture, the concert base is not dray and dielectric permittivity (ε_r = 6)(dielectric permittivity dray concrete ε_r = 5) (Figure 8c), there is some clarity on the radargram, in addition, a correct depth of penetration of the bars is observed, due to of the decrease of the electric conductivity of the concert.

To improve the quality of the radargrams, a signal and image processing on the Reflexw software makes the scans clearer (Figure 9)consequently, this study can be used for might helpful in collection in crucial information about civil engineering.

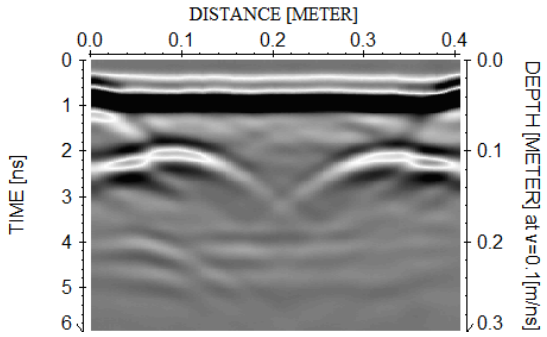

Figure 9: Radargram of the two iron bars
fled in a concrete block, for f =1600MHz after image and signal processing after 21 days

B. *Buried plastic bars in concrete base*

In the second concrete sample, with the same electromagnetic properties, two empty plastic tubes 32 mm in diameter are buried at a depth of 8 cm from the sweeping surface, the distance between them is 300 mm, the slab of concrete is then analyzed every 7 days by radar inspection through a 1600 MHz antenna, the radargrams shown in Figure 10present of hyperbola at depth 8 cm.

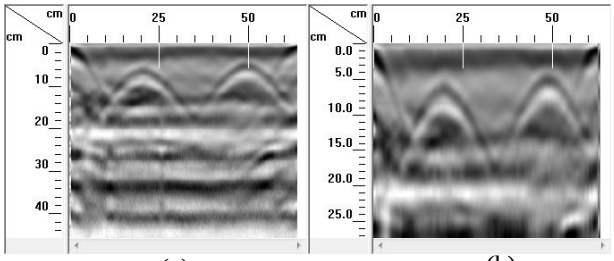

(a) (b)

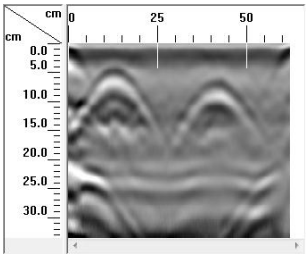

(c)

Figure 10: Radargrams of the two bars of plastic flowing in a concrete block; for f=1600MHz;
(a): experimental with relative permittivity ε_r = 30 (7-day);
(b): ε_r = 15 (14-day); (c): ε_r = 6 (21-day)

Similarly, for the previous experiments results shows that the intensity of the reflection of electromagnetic, depends on the water content of the concrete. In addition, the results become more and more clear due to the decrease in the conductivity. This decrease is strong after 21 days, and the noise in the radargrams schwa with are more clear.

The figure 11 is an approval for the quality improvement of Figure 10 (c) by image processing by reflexw

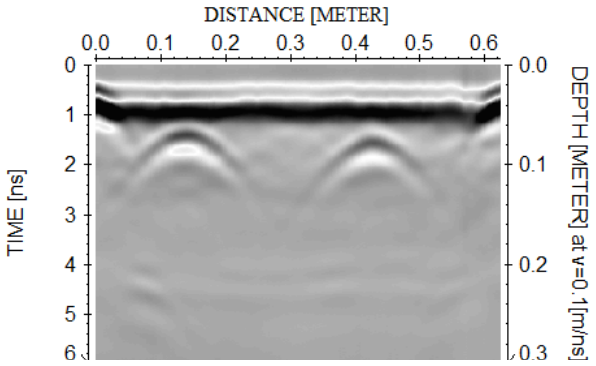

Figure 11: Radargram of the two plastic bars leaking into a concrete block, for f=1600MHz after image and signal processing after 21 days

5. CONCLUSION

The simulation we have achieved for different objects buried (Iron bar, plastic tube and freshwater bottle), GPR radar is through a possesses signal that lets to production of radargrams (B-scan) weir hyperbole that appears indicate the existence of this objects, while given their exact localization in sol depth. We propose in second part, experimental study which in evolve the application of GPR system obtained by experiment. Acquisition experimental data are usually accompanied by treatment to facilitate their interpretation. The GPR experimental data on high water content concrete shows that high hydration increases electromagnetic losses due to increased dielectric constant and conductivity, these losses influence the reflection of the GPR signal and should be taken into account when interpreting GPR data on processed structures. Digital processing, the signals and

images, by the Reflexw software, must be taken into account to improve their quality.

REFERENCES

1. Giannopoulos, A. **The investigation of transmission-line matrix and finite-difference time-domain methods for the forward problem of ground probing radar**. Ph.D. thesis, Department of Electronics, University of York,York, UK ,1997.
2. G. Alsharahi, A. Mint Mohamed Mostapha.**Modelling and Simulation Resolution of Ground Penetrating Radar Antennas**, *Journal of electromagnetic engineering and science* ,2016. https://doi.org/10.5515/JKIEES.2016.16.3.182
3. Yee KS. **Numerical solution of initial boundary value problems involving Maxwells equations in isotropic media**. *IEEE T AntennPropag 1966; 14:49–58.* https://doi.org/10.1109/TAP.1966.1138693
4. G Alsharahi, Ahmed Faize, AM Mohamed Mostapha, AbdellahDriouach.**2D FDTD simulation to Study response of GPR Signals in homogeneous and inhomogeneous mediums**, *International Journal on Communications Antenna and Propagation (IRECAP), 20* ,2016. https://doi.org/10.15866/irecap.v6i3.9276
5. Michael A. Hatch. **The importance of including conductivity and dielectric permittivity information when processing low-frequency GPR and high-frequency EMI data sets**,Elsevier,2013.
6. Ghasemi, Faezeh, Sh, A., Abrishamian, M.S.**A novel method for FDTD numerical GPR imaging of arbitrary shapes based on Fourier transform**. NDT & E Int. 40 (2), 140–146,2007.
7. Millard SG, Shaw MR, Giannopoulos A, Soutsos MN. **Modelling of subsurface pulsed radar for nondestructive testing of structures.***ACSE J. Mater civil Eng.10: 188-196,*1998.
8. Yee KS. **Numerical solution of initial boundary value problems involving Maxwell's equation in isotropic media.***IEEE Transactions on Antenna and Propagation; 14:302,* 1966. https://doi.org/10.1109/TAP.1966.1138693
9. Taflove A**. Review of the formulation and applications of the finite-difference time-domain method for numerical modeling of electromagnetic wave interactions with arbitrary structures**. *Wave Motion; 10:547–82*, 1988.
10. Fernando I. Rial, Manuel Pereira, Henrique Lorenzo. **Resolution of GPR bowtie antennas**, *An experimental approach, Journal of Applied Geophysics 67 367–373* 2009.
11. Alsharahi, Gamil, Ahmed Faize, Carmen Maftei, and AbdellahDriouach. **GPR Application for Risks Detection in Subsurface Engineering Construction Projects.***Ovidius University Annals of Constanta-Series Civil Engineering* 21, no. 1, 51-58, 2019. https://doi.org/10.2478/ouacsce-2019-0006
12. Alsharahi, G., A. Faize, M. Louzazni, A. M. M. Mostapha, M. Bayjja, and A. Driouach. **Detection of cavities and fragile areas by numerical methods and GPR application.***Journal of Applied Geophysics p 164, 225-236,* 2019.
13. Alsharahi, Gamil, Ahmed Faize, Carmen Maftei, Mohamed Bayjja, Mohamed Louzazni, AbdellahDriouach, and AbdellatifKhamlichi**. Analysis and Modeling of GPR Signals to Detect Cavities: Case Studies in Morocco.***Journal of Electromagnetic Engineering and Science 19,* no. 3, p177-187, 2019. https://doi.org/10.30534/ijeter/2019/11782019
14. Annan, A. P. **Ground penetrating radar workshop notes.***Mississauga, Ontario, 128 p,*1992.
15. MouradAdous.**Electromagnetic characterization of civil engineering treated metals in the frequency band 50 MHz - 13 GHz.** Ph.D thesis, University Nantes05 octobre 2006.
16. Aaron Don M, Antonio Miguel Sarmiento Alejo, Grant Lewis Milan Bulaong, Samantha Maxine Ronquillo Santos, Jerrick Spencer KehyengUy. **Effect of Dielectric Substrate on Dipole Antenna Directivity,** *International Journal of Emerging Trends in Engineering Research,*volume 7, No.8 August 2019.
17. S. Trehubenko, L. Berkman, N.Yeromina, S. Petrov, Y. Bryzhatyi, H. Kovalov, V. Dachkovskyi, L. Mikhailova. **The Operation of Detection Systems in Conditions of Contrast Decrease of Ground Objects,** *International Journal of Emerging Trends in Engineering Research,* volume 8, No.1, January 2020. https://doi.org/10.30534/ijeter/2020/28812020